European Journal of Pharmaceutics and Biopharmaceutics 134 (2019) 96–106

Contents lists available at ScienceDirect

European Journal of Pharmaceutics and Biopharmaceutics

journal homepage: www.elsevier.com/locate/ejpb

Research paper

Prevention of hepatic stellate cell activation using JQ1- and atorvastatin-loaded chitosan nanoparticles as a promising approach in therapy of liver fibrosis

Raghda Hassan[a], Salma N. Tammam[a,*], Sara El Safy[a], Mohammad Abdel-Halim[b], Anastasia Asimakopoulou[c], Ralf Weiskirchen[c], Samar Mansour[a]

[a] Department of Pharmaceutical Technology, Faculty of Pharmacy & Biotechnology, The German University in Cairo (GUC), Cairo, Egypt
[b] Department of Pharmaceutical Chemistry, Faculty of Pharmacy & Biotechnology, The German University in Cairo (GUC), Cairo, Egypt
[c] Institute of Molecular Pathobiochemistry, Experimental Gene Therapy and Clinical Chemistry (IFMPEGKC), RWTH University Hospital Aachen, Aachen, Germany

ARTICLE INFO

Keywords:
Liver fibrosis
Active targeting
Hepatic stellate cells
Targeting ligand density
Atorvastatin
JQ1

ABSTRACT

Preventing hepatic stellate cell (HSC) activation represents a promising approach to resolve liver fibrosis. Several drugs have been reported to delay/prevent HSCs activation, however with limited clinical benefits. The latter may be in part attributed to the limited ability of such drugs in targeting more than one pathway of HSC activation. Added to that, is their inability of reaching their target cell in sufficient amounts to induce a therapeutic effect. In this work, chitosan NPs were loaded with JQ1 and atorvastatin, two drugs that have been reported to prevent HSCs activation, however via different mechanisms. NPs were then modified with different densities of retinol (Rt) for active targeting of HSCs. The NP HSCs targeting ability as a function of Rt density was assessed *in vitro* on primary HSCs and *in vivo* in carbon tetrachloride (CCl_4) induced fibrotic mouse models. *In vitro* NPs modified with a low Rt density (LRt-NPs) showed ≈2 folds enhanced HSCs uptake in comparison to unmodified NPs, whereas NPs modified with a high Rt density (HRt-NPs) showed ≈0.8 folds change in uptake relative to unmodified NPs. Similarly, *in vivo* LRt-NPs showed higher accumulation in fibrotic livers in comparison to healthy livers whereas HRt-NPs and unmodified NPs showed lower accumulation in fibrotic livers relative to healthy controls respectively. Finally, the ability of drug-loaded NPs in preventing HSCs activation was assessed by monitoring the reduction in α-smooth muscle actin (α-SMA) expression by Western blot. NPs loaded with both JQ1 and atorvastatin showed reduction in α-SMA expression. In addition, a synergistic reduction in α-SMA was observed when cells were co-treated with JQ1 and atorvastatin loaded NPs.

1. Introduction

The development of fibrotic tissue in the liver occurs in response to injury [1], in which the injured tissue is replaced by a collagenous scar [2]. When injury persists, fibrosis ultimately concludes in cirrhosis that is usually accompanied by a wide spectrum of complications, including portal hypertension, liver failure and hepatocellular carcinoma [3].

A cascade of events culminates in the formation of the fibrotic scar. The main players of such cascade are the hepatic stellate cells (HSCs) [3,4]. Under normal conditions, HSCs are quiescent, retinoid -containing stromal cells located between the sinusoidal endothelium and hepatocytes in the space of Disse [5,6]. However, in response to liver injury, they become activated. Activated hepatic stellate cells (aHSCs) secrete transforming growth factor (TGF)-β1, which induces collagen production leading to excessive extracellular matrix (ECM) deposition and accumulation. Additionally, aHSCs inhibit matrix metalloproteinases (MMPs) via the up-regulation of tissue inhibitors of metalloproteinases (TIMPs), which eventually results in reduced ECM degradation

Abbreviations: ANOVA, One way analysis of variance test; At, Atorvastatin; BET, Bromodomain and extraterminal; BRD4, Bromodomain-containing protein 4; CDI, 1,1′-Carbonyldiimidazole; DMSO, Dimethyl sulfoxide; ECM, Extracellular matrix; FL, Fluorescein; HCV, Hepatitis C virus; HD, Hydrodynamic diameter; HEK 293, Human embryonic kidney cell line; HRt-NPs, High Rt density; HSC, Hepatic stellate cell; IP, Intra-peritoneal; IV, Intra-venous; LRt-NPs, Low Rt density,; LSECs, Liver sinusoidal endothelial cells; NAFLD, Nonalcoholic fatty liver diseases; NPs, Nanoparticles; PBS, Phosphate buffered saline; RBP, Retinol binding protein; RES, Reticuloendothelial system; Rt, Retinol; SEM, Scanning electron microscopy; TGF-β1, Transforming growth factor; TIMPs, Tissue inhibitors of metalloproteinases; TPP, Sodium tripolyphosphate; α-SMA, f α-smooth muscle actin

* Corresponding author.
E-mail address: salma.nabil@guc.edu.eg (S.N. Tammam).

https://doi.org/10.1016/j.ejpb.2018.11.018
Received 18 June 2018; Received in revised form 9 October 2018; Accepted 20 November 2018
Available online 22 November 2018
0939-6411/

[3,4]. Activation of HSCs occurs over two stages; initiation and perpetuation [1]. Initiation is mainly brought about by paracrine stimulation from neighboring hepatocytes, endothelial and Kupffer cells, in addition to platelets. Perpetuation on the other hand, involves both autocrine and paracrine loops [1]. For such reasons, preventing HSC activation and the consequent reduction of the activated phenotype represents a promising approach to resolve liver fibrosis [7].

Apart from their well-known role as antilipidemic drugs, statins have proven to be of value in the prevention of HSC activation. *In vitro*, statins have shown the ability to inhibit HSC proliferation [8]. Early treatment with atorvastatin after bile duct ligation in rats attenuated activation of HSCs and subsequent collagen deposition [9]. More recently, statins were reported to be associated with a reduced risk of fibrosis progression in chronic Hepatitis C virus (HCV) infection [10]. Interestingly, statins have also been reported to decrease hepatic venous pressure and improve liver perfusion in patients with cirrhosis [11].

Bromodomain-containing protein 4 (BRD4), is a bromodomain and an extraterminal (BET) family member. BET proteins regulate transcription of genes involved in several functions including apoptosis, cell cycle progression, inflammation, among others [12]. BRD4 seems to play a critical role in fibrosis, where BDR4 enhancers mediate profibrotic gene expression in HSCs [5]. Blocking of BRD4-enhancer interactions is therefore expected to reduce HSC activation. JQ1 is a small molecule inhibitor of BRD4, which has recently been reported to abrogate cytokine-induced activation of HSCs and reverse the fibrotic response in animal models [5]. It is however worth noting that, BRD4 is involved in a myriad of biological processes including memory formation, mitochondrial oxidative phosphorylation, and DNA damage response, and many other biological processes [13–15]. For such reason, the general inhibition of BRD4 would not be free of adverse off-target effects [16–18].

Nanoparticles (NPs) have developed a reputation for their ability to deliver drugs specifically to their site of action; drug targeting [19]. The latter offers means for the administration of pharmaceutical interventions that show promising therapeutic effects, but their clinical use is unfortunately hampered by insufficient supply of drugs to the diseased target tissue and/or by undesirable off-target effects [19,20]. For drug targeting to HSCs, the NPs should initially allocate to the liver, and in the liver subsequently show an increased uptake by HSCs. In healthy livers, the liver sinusoidal endothelial cells (LSECs) fenestrae are organized in typical sieve plates and measure ≈50–250 nm in diameter [21,22]. These fenestrations are believed to facilitate the transport of macromolecules from the sinusoidal lumen, into the space of Disse [23]. Theoretically, NPs are expected to translocate into the liver using the same mechanism. Decreased fenestrae formation and diameter are observed in LSEC in fibrotic livers [23–25]. The latter makes it harder for NPs that under normal conditions would have gained access into the liver, to do so in fibrotic livers. Smaller NPs would however have a larger chance of translocating into the liver. The retinol binding protein (RBP) receptor is implicated in the storage of retinol in quiescent HSCs and therefore serves an interesting receptor for NP HSC targeting [20]. Once in the liver, small NPs modified with retinol as a targeting ligand should preferentially allocate to HSCs delivering their drug load to their target cell.

In this work, small chitosan NPs loaded with JQ1 and atorvastatin that were modified with different densities of retinol as a targeting ligand are used for drug targeting to quiescent HSCs with the aim of preventing their activation. The effect of retinol density as a targeting ligand on the extent of HSCs uptake and the consequent ability of NPs to prevent HSCs activation was assessed *in vitro* on primary quiescent HSCs. The *in vivo* liver allocation of NPs as a function of Rt density was also determined in healthy and liver fibrosis animal models.

2. Methodology

2.1. Nanoparticle preparation and characterization

2.1.1. Void unloaded NPs

Void unloaded Chitosan NPs were formulated by the inotropic gelation method as detailed in earlier work [26]. Briefly, in a ratio of 1:1, 0.125% (w/v) sodium tripolyphosphate (TPP; Mistral Chemicals UK) was added to 0.5% (w/v) chitosan (Low Molecular weight, Sigma Aldrich) dissolved in 1% acetic acid, pH 4 and stirred for 30 min at 1000 rpm. NP average hydrodynamic diameter (HD) was measured using a Malvern Zetasizer Nano ZS90 (Malvern Instruments Ltd, Malvern, UK). Three batches of NPs were prepared and each analyzed in triplicates at 25 °C. Results were expressed as mean ± standard deviation (SD).

For morphological analysis, a drop of the NP suspension was spread on a Silicon wafer and subjected to field-emission scanning electron microscopy (SEM) using a LEO SUPRA 55 microscope (Carl Zeiss, Reutlingen, Germany).

The number of NPs in 1 mL NP suspension was calculated from the mean HD as detailed in earlier work [26]. Briefly, NP number was calculated using equations 1–3 as follows:

Volume of polymer used in NP formulation = mass of polymer used in NP formulation /density of polymer (1)

Volume of NP = $4/3\,\pi\,r^3$ (2) where r is the NP radius

No. of NPs = Volume of polymer used in NP formulation/volume of one NP (3)

2.1.2. Nanoparticle drug loading

(+)-JQ-1 (MedChemExpress, Monmouth Junction, NJ, USA) was dissolved in dimethyl sulfoxide (DMSO) at a concentration of 4 mg/mL. Atorvastain calcium salt was a kind gift from EPICO Pharmaceuticals Cairo, Egypt. Atorvastatin (At) was dissolved in methanol at a concentration of 10 mg/mL. Drug loaded NPs were prepared in a similar manner to void NPs, however, 50 µL of drug solution in DMSO or methanol for JQ1 and atorvastatin respectively, were added to the chitosan solution prior to TPP addition.

To determine the encapsulated drug concentration in chitosan NPs, NPs were centrifuged at 14,000*g* for 30 min. The concentration of un-encapsulated drug in the supernatant was determined for both drugs. Consequently, the encapsulated concentration was determined indirectly by subtracting the un-encapsulated drug concentration in the supernatant from the total concentration of drug added.

For JQ1, unencapsulated drug was quantified in the supernatant by spectrophotometry at ʎ254nm. Un-encapsulated At concentration in the supernatant was determined by an in-house developed UPLC-MS/MS method. Method details and validation are provided in the supplementary information file. The developed method was performed using simvastatin as internal standard. Analyses were acquired on a Waters ACQUITY Xevo TQD system, which consisted of ACQUITY UPLC H-Class system and XevoTQD triple-quadrupole tandem mass spectrometer with an electrospray ionization (ESI) interface (Waters Corp., Milford, MA, USA). CORTECS C18 50 mm × 2.1 mm column (particle size: 2.7 µm) was used to separate analytes (Waters, Wexford, Ireland). System operation and data acquisition were controlled using MassLynx 4.1 software (Waters). All data were processed with the TargetLynx quantification program (Waters).

For both drugs encapsulation efficiency was determined form at least three independently prepared batches, each analyzed in duplicates. Results were expressed as mean ± SD.

2.2. Nanoparticle hemocompatibility

2.2.1. Determination of NP hemolytic potential

To determine whether chitosan NPs induce hemolysis upon intravenous administration, 10 mL whole blood was collected in

lavender-top – EDTA tubes. To 500 µL of whole blood, increasing NP concentrations (50, 100, 200, 400, and 800 µg/mL) were added. Phosphate buffered saline (PBS) was used as negative control. Blood samples spiked with PBS and subjected to sonication in a water bath sonicator for 30 min were used as a positive control. Samples and controls were incubated for 2 h in a shaking water bath maintained at 37 °C. After incubation, samples and controls were centrifuged at 4000*g* for 10 min and supernatants were assayed by spectrophotometry at ʎ540 nm [27]. Percent of hemolysis induced by NPs was calculated as detailed in [27]. Experiment was conducted in duplicates and results expressed as mean ± SD.

2.2.2. Determination of NP RBC agglutination potential

The ability of the NPs to induce agglutination upon intravenous administration was determined using the saline agglutination test [28]. Briefly, a drop of NP suspension at increasing concentrations (50, 100, 200, 400, and 800 µg NPs/mL) were placed on a glass slide. One drop of whole blood was added to each of the NPs and observed for the presence of agglutination macroscopically and under a light microscope. A drop of 0.9% saline was used as a control.

2.3. Nanoparticle modification with retinol as a targeting ligand and quantification of retinol density on the NP surface

A 1 mL aliquot of 5 mg/mL retinol (Rt; Sigma Aldrich, Taufkirchen, Germany) in DMSO was added to 0.5 mL of 12 mg/mL 1,1′-Carbonyldiimidazole (CDI, Sigma Aldrich) in DMSO, mixed and incubated overnight in a shaking incubator yielding Rt-CDI solution. NPs were prepared as detailed earlier and centrifuged at 14,000*g* for 30 min. Supernatants were discarded, and NPs were reconstituted in de-ionized water. To 0.5 mL NP aliquots, increasing concentrations of Rt-CDI were added; 60, 80, 100 and 150 µg/mL and incubated overnight in a shaking incubator. To determine the density of Rt bound to the NP surface. Retinol-modified NPs (Rt-NPs) were centrifuged at 14000*g* for 30 min, supernatants discarded, and Rt-NP pellets were reconstituted in de-ionized water. Rt concentration was determined by fluorometry ʎexc:335 nm and ʎem:448 nm. For all Rt concentrations, three independent NP aliquots were modified with Rt. The fluorescence intensities were determined in single for each aliquot and results were expressed as mean ± SD. The concentration of tagged retinol per mL NPs, the number of NPs/mL NP suspension in addition to the NP HD were used to calculate the number of Rt molecules per nm^2 as detailed in earlier work [26].

2.4. Primary quiescent hepatic stellate cell isolation and characterization

The standardized method for isolation of murine hepatic stellate cells was reported before [29]. In brief, murine livers were enzymatically digested with pronase and collagenase, and enriched by centrifugation of the crude cell suspension through a Nycodenz gradient. For the study presented here, we used cells that were not further purified by FACS sorting. Using this protocol, the obtained cell yield is approximately 1–2 × 10^6 HSC per mice having a viability of 75–80% and a purity of approximately 80–85%. All reagents used in this protocol and the methods to determine vitality and purity are given elsewhere [29].

2.5. Nanoparticle uptake as function of retinol density in quiescent hepatic stellate cells and HEK293 cells

Chitosan NPs were loaded with fluorescein (FL; Sigma Aldrich), in a similar manner to At, where FL was initially dissolved in methanol, following which 50 µL of the FL solution were added to the chitosan solution prior to TPP addition. To determine the effect of Rt density on the extent of NP uptake by quiescent HSCs, FL-loaded NPs were modified with either a low density (60 µg/mL) or a high (100 µg/mL) density of Rt (LRt-NPs and HRt-NPs respectively). In two 96 well plates, freshly isolated quiescent HSCs were seeded at a density of 10^4 cell/well. In the first plate, unmodified FL loaded NPs, and FL loaded LRt-NPs and HRt-NPs were added to cells at a concentration of 49 and 67 µg/mL. NPs were incubated with cells for 24 h, following which NP containing medium was aspirated. Cells were washed twice with PBS. The extent of NP uptake was determined by fluorometry ʎexc:490 nm and ʎem:520 nm using NP curves as detailed in earlier work [26,30]. The experiment was repeated using the second plate of HSCs, however NPs were added to cells after the cells had been in culture for 4 days. As a control cell line, NP uptake experiment was also repeated in human embryonic kidney cell line HEK293 [31]. Results were expressed as mean ± SD for n = 4.

2.6. Determination of the ability of NPs to prevent activation of quiescent HSCs- quantification of α-SMA expression

The determination of the NP ability to prevent activation of quiescent HSCs was conducted by Western blot using α-SMA expression as read out system. HSCs were seeded in 6 well plates (2 × 10^5 cells per well) and were treated one day after seeding with drugless unloaded NPs (both unmodified and Rt modified) at a low (49 µg/mL) or high concentration (67 µg/mL). Cells were also treated with drug loaded NPs, for JQ1, cells were treated with 1 and 10 µM of JQ1 loaded NPs (in terms of encapsulated JQ1) and for At cells were treated with 10 and 20 µM of At loaded NPs (in terms of encapsulated At). Drug concentrations used were chosen according to work conducted by Ding et al. [5] and Klein et al. [32] for JQ1 and At, respectively. Concentrations of unloaded NPs tested corresponded to the lowest and highest concentration of drug loaded NPs used in terms of polymer concentration.

Four days after seeding, the cells were re-stimulated with new NPs similarly as on day one. On day seven after seeding (3 days after the second round of treatment), cells were harvested. Preparation of cellular protein extracts and conditions used for Western blot analysis were described previously [33]. Equal loading of lanes was demonstrated by probing with an antibody specific for glyceraldehyde 3-phosphate dehydrogenase (GAPDH). Antibodies used were α-SMA (CBL171, Cymbus Biotech, Hampshire, UK) and GAPDH (sc-32233, Santa Cruz Biotech., Santa Cruz, CA, USA). Densitometric analysis was also performed to verify the Western blot outcome using the LumiAnalyst software (version 3.1) and the Lumi-Imager system (both from Roche Diagnostics, Mannheim, Germany). Band intensities were normalized to the GAPDH signals. The control band intensity was set to 1 and the other intensities were given as fold induction.

2.7. NP in vivo liver accumulation as function of retinol density in healthy and fibrotic livers

Twenty male Swiss albino mice (8 weeks old, weighing 25–30 g) were purchased from Theodor Bilharz Research Institute (TBRI) Cairo, Egypt. Mice were divided into two groups. In the first group, liver fibrosis was induced by intra-peritoneal (IP) injection of 10% CCl_4 in olive oil (2.5 mL per kg body weight) twice a week for 4 weeks [34]. To confirm the establishment of fibrosis, after 4 weeks of CCl_4 injections, one mouse was sacrificed by cervical dislocation and liver tissue samples were obtained, for histopathological investigations. The second group served as the healthy controls and received the same volume of olive oil though IP injections.

For histopathological investigations autopsy samples were obtained from the liver and fixed in 10% formol-saline fixative for 24 h. Washing was conducted in tap water then serial dilutions of alcohol (methyl, ethyl and absolute ethyl) were used for dehydration. Specimens were cleared in xylene and embedded in paraffin at 56 °C in a hot air oven for 24 h. Paraffin bees wax tissue blocks were prepared for sectioning at 4 µm thickness by a sledge microtome. The obtained tissue sections

were collected on glass slides, deparaffinized, stained by hematoxylin and eosin stain for examination through the light electric microscope

Each group was further divided into 3 sub-groups each composed of 3 mice. These subgroups were either injected with FL loaded unmodified NPs, LRt-NPs or HRt-NPs IV through the tail vein. Control groups received the same volume of PBS also through the tail vein.

Prior to administration, NPs were centrifuged and reconstituted in PBS at a NP concentration of 13.6 mg/mL in terms of polymer concentration. A total of 0.8 mg NPs were administered intravenously through the tail vein per mouse. The total NP amount was divided over 4 doses given at 2 h intervals. One hour after the last dose, the mice were sacrificed by cervical dislocation and liver tissue samples were obtained. Livers were homogenized in PBS to yield a homogenate with a final concentration of 0.25 mg/mL. Liver homogenates prepared from mice that have not been injected with NPs were prepared in a similar manner and used to establish NP curves, where a serial dilution of FL loaded unmodified, LRt-NPs and HRt-NPs were prepared in liver homogenates. These curves were used to determine the NP concentration in NP treated liver homogenates.

Animal care and all experimental procedures were conducted according to ethical guidelines of the Research Ethics Committee of Faculty of Pharmacy; German University in Cairo (GUC).

2.8. Statistical analysis

Statistical analysis was performed by GraphPad InStat software (GraphPad Software, La Jolla, CA, USA) using one way analysis of variance test (ANOVA), where $P < 0.05$ was considered significant, $P < 0.01$ was considered very significant, and $P < 0.001$ was considered extremely significant.

3. Results

3.1. Nanoparticle preparation and characterization

NPs formed spontaneously upon addition of TPP to chitosan. SEM analysis shows that the NPs are spherical in shape and unaggregated (Fig. 1). NPs had HD of 99 ± 22 nm. Supplementary Fig. S1 shows the NP HD distribution chart. NPs were successfully loaded with drug, JQ1 NPs contained 16.5 ± 1.7 μg/mL JQ1, whereas atorvastatin NPs contained 67.4 ± 5 μg/mL atorvastatin. Supplementary Figs. S2 and S3 show UPLC-MS/MS chromatogram of At and simvastatin respectively.

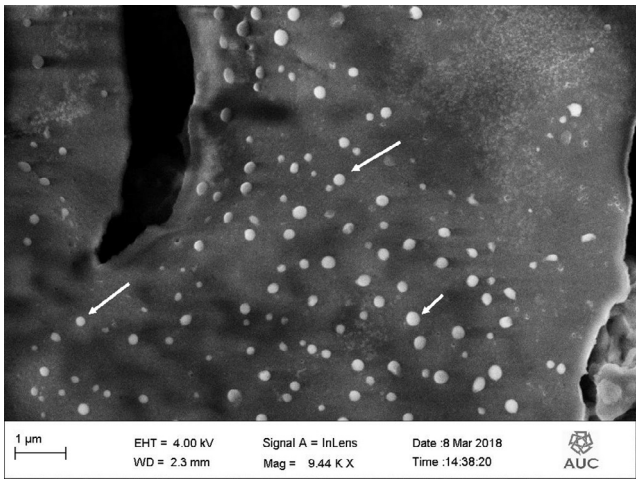

Fig. 1. Scanning electron microscopy of chitosan NPs. Arrows point to particles showing typical chitosan NP appearance.

3.2. Nanoparticle hemocompatibility

Fig. 2 shows results obtained when increasing concentrations of NPs were incubated with whole blood. When incubated with whole blood NPs did not induce significant hemolysis up to 400 μg/mL. At 800 μg/mL NPs induced around 10% hemolysis. As for RBC agglutination, NPs did not cause any agglutination up to 800 μg/mL either macroscopically or following investigation under a light microscope. Supplementary Fig. S4, shows microscopic images of unagglutinated RBC observed with NP free controls and with 800 μg/mL NP-blood samples.

3.3. Nanoparticle modification with retinol as a targeting ligand and quantification of retinol density on the surface of NP surface

Fig. 3 shows the increase in density of Rt tagged onto the NP surface with the increase in concentration of Rt added. Accordingly, a Rt density of ≈40 μg/ml and 60 μg/mL tagged Rt were considered low Rt density (LRt) and high Rt density (HRt) respectively. Accordingly, LRt-NPs have ≈0.59 Rt molecules per nm^2 whereas HRt-NPs have ≈0.86 molecules per nm^2.

3.4. Primary quiescent hepatic stellate cell isolation and characterization

To analyze the uptake of NPs in HSC, primary murine hepatic stellate cells were isolated from wild type mice. For the experiment depicted in Fig. 4, the isolated cells had an overall purity of 82% and a vitality of 96%.

3.5. Nanoparticle uptake as function of retinol density in quiescent hepatic stellate cells and HEK293 cell

Fig. 4 shows the extent of NP uptake as a function of Rt density in primary quiescent HSCs and HEK 293 cells. In both cell types, NPs showed a concentration-dependent uptake, with an overall higher extent of uptake in primary quiescent HSCs (Fig. 4A) in comparison to HEK 293 cells (Fig. 4 B). The difference in the extent of uptake is most prominent in LRt-NPs at a higher NPs concentration. Given their Rt uptake capacity, when treated with the higher NP concentration (67 μg/mL) primary quiescent HSCs show ≈2.7 folds higher uptake of LRt-NPs in comparison to HEK 293 cells.

Fig. 4C and D, show the folds change in extent of Rt-NPs uptake relative to unmodified NPs in HSCs and HEK293 cells respectively. When primary HSCs that have only been cultured in 96 well plates for 2 days were treated with 67 μg/mL LRt-NPs and HRt-NPs, LRt-NPs showed ≈1.9 folds increase in uptake relative to unmodified NPs, whereas HRt-NPs showed no increase in uptake relative to unmodified NPs (Fig. 4C). Such difference in uptake was only obvious in primary HSCs and not in HEK 293 cells (Fig. 4D). Additionally, when primary HSCs were cultured in 96 well plates for 4 days prior to NP-cell incubation, the extent of LRt-NPs uptake was reduced, where LRt-NPs did not show any significant increase in uptake relative to unmodified NPs (Fig. 4C).

3.6. Determination of the ability of NPs to prevent activation of quiescent HSCs- quantification of α-SMA expression

Fig. 5 shows the NPs' ability in preventing the activation of quiescent HSCs using α-SMA expression as readout. Fig. 5A shows results obtained with unloaded drugless NPs, when HSCs were incubated with a low (49 μg/mL) and a high (67 μg/mL) concentration of unloaded, unmodified NPs, and unloaded LRt-NPs and HRt-NPs. In Fig. 5A results for Rt modified NPs were normalized to those obtained with unmodified NPs. At 67 μg/mL unloaded HRt-NPs reduced α-SMA protein levels indicating reduced activation of quiescent HSCs. Fig. 5B shows results obtained with drug loaded LRt-NPs. Reduction in α-SMA expression was observed in a concentration dependent manner when cells

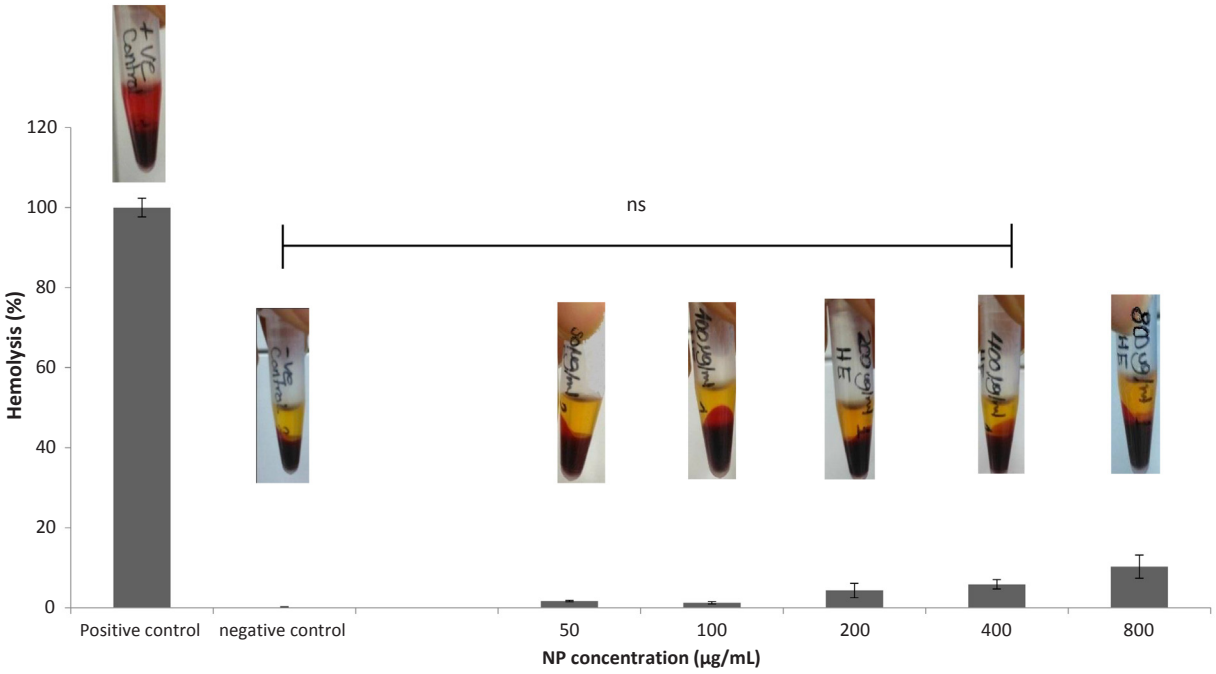

Fig. 2. Determination of the chitosan NP hemolytic potential. Up to 400 µg/mL chitosan NPs do not induce hemolysis.

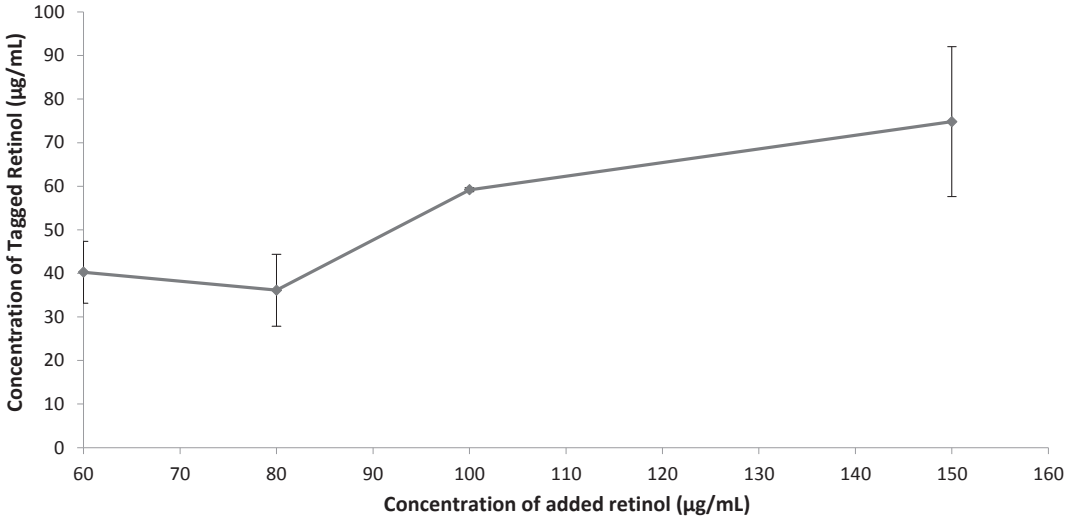

Fig. 3. Quantification of the density of retinol tagged onto the nanoparticle surface.

were treated with 1 and 10 µM of JQ1 NPs and 10 and 20 µM At NPs in addition to a combination of 10 µM JQ1 + 20 µM At NPs. Co-treatment with 10 µM JQ1 + 20 µM At NPs showed a synergistic reduction in α-SMA expression. At the same concentrations, treatment with free drugs was not possible due to cytotoxicity. Supplementary Fig. S5 shows results obtained with JQ1 and At unmodified and HRt-NPs. Although these NPs do not provide highest uptake in HSCs drug loaded NPs still show a reduction in α-SMA expression.

3.7. NP in vivo liver accumulation as function of retinol density in healthy and fibrotic livers

Fig. 6A confirms the establishment of fibrosis with CCl_4 administration. In particular, it shows inflammatory cells infiltration with fibroblastic cells proliferation originating from the portal area and extended in between the hepatocytes of the parenchyma associated with multiple newly formed bile ductules in the portal area as well as karyomegaly in the nuclei of some hepatocytes. Fig. 6B shows NP liver accumulation profiles in fibrotic and healthy mice. Interestingly, while LRt-NPs are undetectable in the livers of healthy mice, they show high accumulation in fibrotic mice. While unmodified NPs and HRt-NPs show a 0.8 and 0.9 fold reduction in liver accumulation in fibrotic livers relative to healthy livers, LRt-NPs show a 1.8 fold increase in accumulation in fibrotic livers relative to healthy ones.

4. Discussion

Most antifibrotic strategies in current development focus on cell-extrinsic signaling molecules, or receptors required for profibrogenic signaling pathways [5]. Given the pivotal role played by HSCs in the fibrotic process, targeting the HSCs themselves and preventing their activation is a promising approach to resolve liver fibrosis. Notwithstanding, given the complexity of the mechanisms behind HSC activation and perpetuation [1], it has become obvious that therapeutic

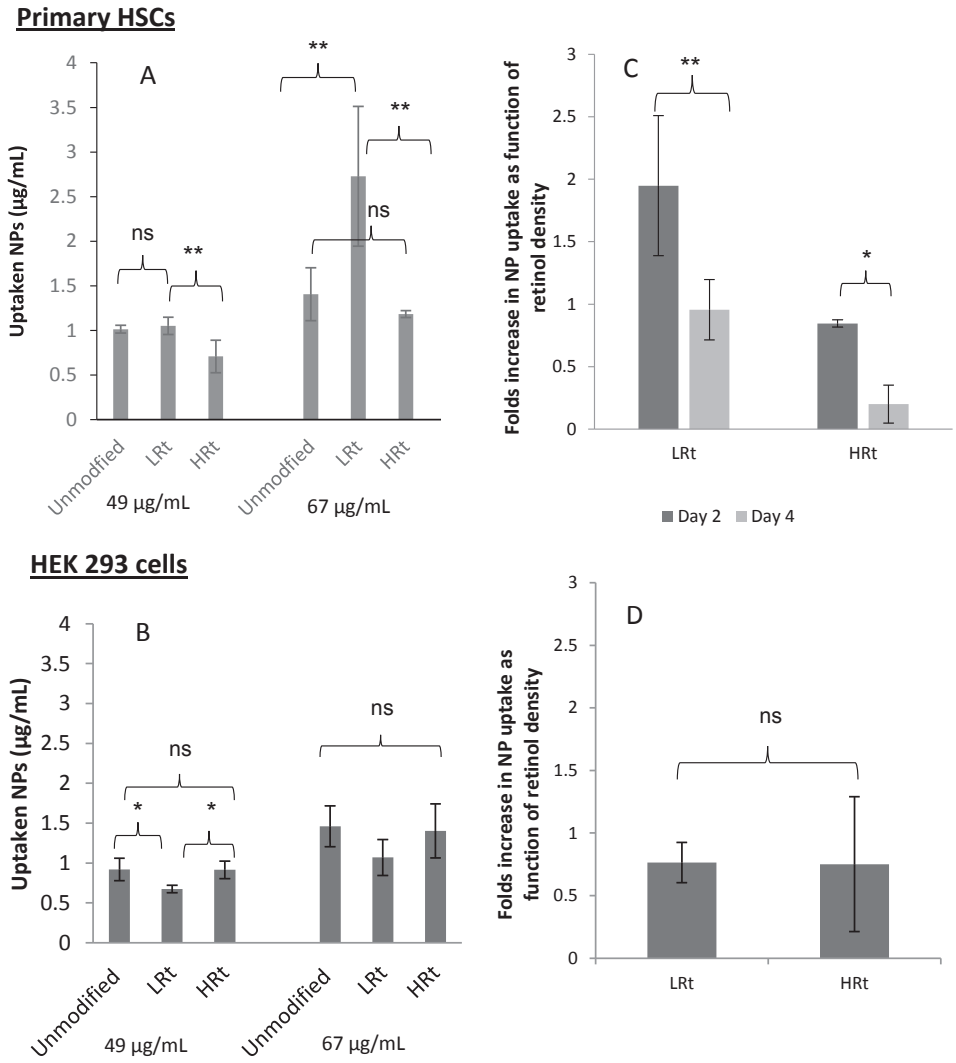

Fig. 4. NP uptake as function of retinol density in (A) primary HSCs and (B) HEK 293 cells. (C, D) show fold changes in extent of uptake of retinol- modified NPs in comparison to unmodified NPs in (C) HSCs at 2 and 4 days of culture and in (D) HEK293 cells. ***extremely significant, **very significant, *significant, ns: not significant.

interventions working at one end only might not be sufficient. In fact, the limited clinical benefits seen with most traditional antifibrotic therapies might in part be attributed to their limited ability of targeting more than one pathway [5]. Added to that, is their inability of reaching their target cell (when administered in a safe dose) in sufficient amounts to induce a therapeutic effect [35,36]. In such case, targeting of HSCs by more than one drug that ultimately lead to the same final therapeutic outcome, however via different pathways, might have a synergistic therapeutic outcome.

For successful targeting of HSCs by NPs in liver fibrosis, the NPs are initially expected to reach the liver, following which preferentially allocate to the HSCs. Given the liver's high perfusion, the intravenous route presents an interesting means for the delivery of NPs to the liver. Upon intravenous administration, the process of NP opsonization and protein corona formation dictates the NP fate [19,37,38]. It is generally agreed upon that hydrophobic NPs that are larger than ≈200 nm tend to be opsonized by proteins that render them attractive to the phagocytic cells of the reticuloendothelial system (RES). These NPs are rapidly up-taken from the circulation and accumulate in circulating macrophages, Kupffer cells of the liver and resident phagocytic cells of the spleen [19,36,39]. Smaller more hydrophilic NPs tend to have longer circulation times and hence have a larger chance in reaching the liver vasculature. Once in the liver, their size is one of main factors dictating their ability to gain access into the space of Disse. Given the capillarization occurring in fibrotic livers, it is quite possible that highly fibrotic areas of the liver might not be readily accessible to NPs [35]. However, smaller NPs will have a higher chance in gaining access to the space of Disse in areas where fenestrae are still somehow accessible.

Chitosan is a hydrophilic polymer which has been reported to show stealth properties and evade the sequestration by the reticuloendothelial systems (RES) when NPs are formulated in the correct size [40]. In this study, NPs prepared were ≈100 nm in diameter to firstly enable evasion of RES sequestration and to be able to access the space of Disse *via* the remaining fenestrae. Other NP-based formulations were also developed with the aim of HSCs targeting. What is common to most of them is the selected NP diameter being in the range of ≈100 nm [35,41–44]. However, it is worth noting that for those particles prepared from hydrophobic materials, increasing hydrophilicity by PEGylation was necessary to avoid RES sequestration [42,43], since hydrophobic particles of the same size range were shown to be taken-up by other macrophages, particularly in the lung [35]. Lung accumulation of such particles is usually enhanced due to the abnormal pulmonary reticuloendothelial uptake occurring in cirrhosis [45]. Although NP PEGylation will increase NP circulation time, thereby increasing its chances in allocating to the liver, PEGylation has unfortunately been reported on numerous occasions to reduce NP-cell interaction,

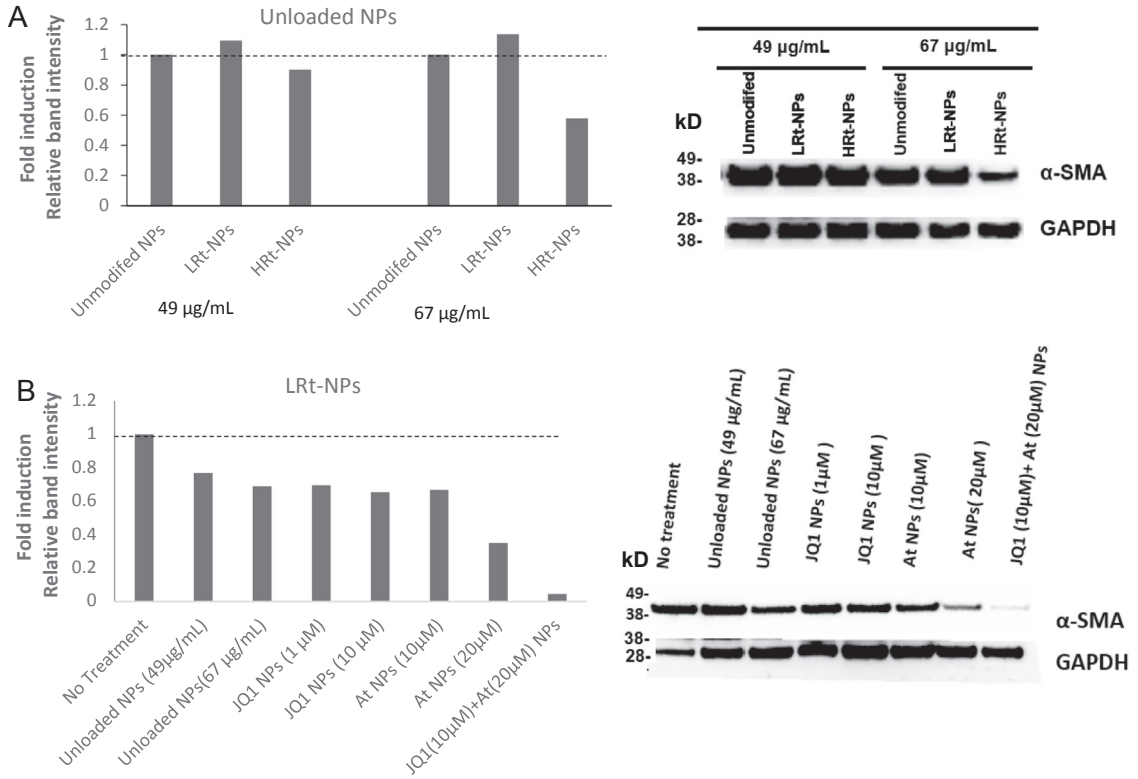

Fig. 5. NP ability in reducing α-SMA expression in primary HSCs. (A) Reduction in α-SMA expression as a function of treatment with unloaded drugless NPs modified with different densities of Rt. (B) Reduction in α-SMA expression as a function of treatment different concentrations of JQ1 and Atorvastatin loaded LRt-NPs.

consequent uptake and targeting ability [46–48]. Hence, other approaches to stealth NPs would be more favorable. Larger particles also intended for HSC targeting exhibited significant accumulation in the lung, and spleen [49,50]. In the case where the therapeutic molecule delivered shows specificity of action to HSCs the latter would not be problematic [49]. However, in cases where drug specificity was not possible, these NPs would unfortunately exacerbate the dilemma of off-target drug effects.

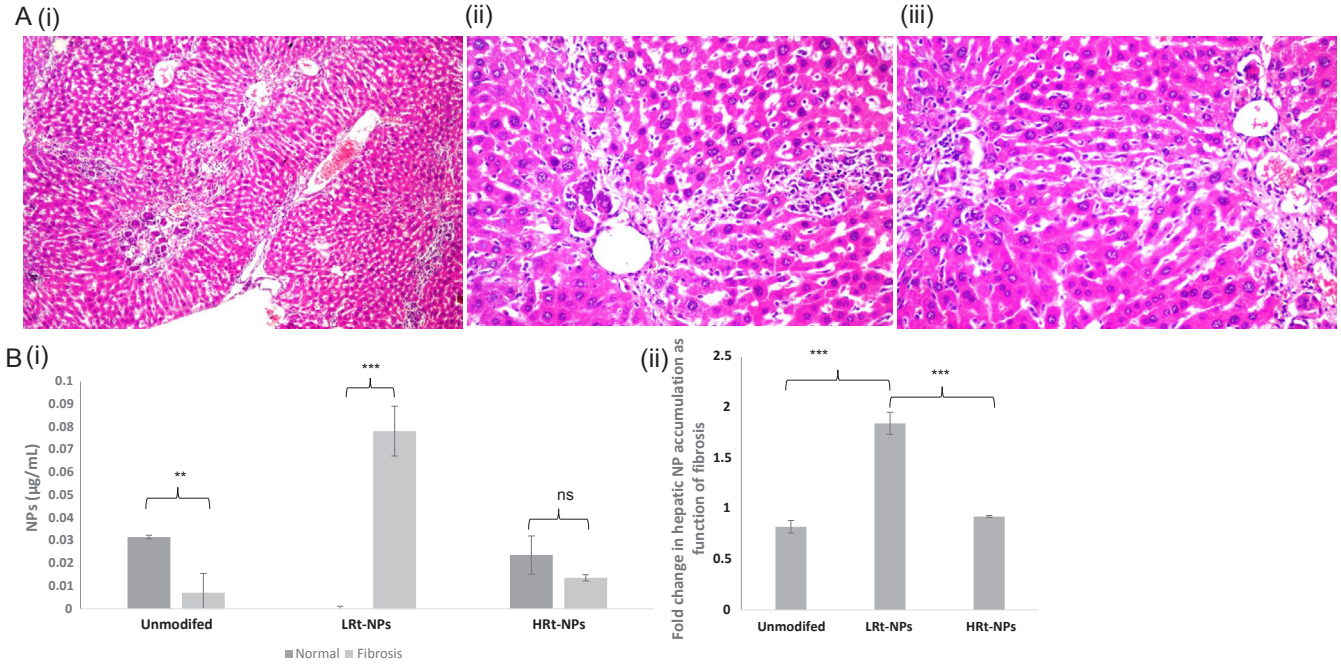

Fig. 6. (A) Microscopic images showing histopathological features of liver sections obtained from a fibrotic mouse receiving intra-peritoneal (IP) injection of 10% CCl4 in olive oil (2.5 mL per kg body weight) twice a week for 4 weeks. (i) 40× magnification, (ii)and (iii)both at 80× magnification (B) In vivo NP liver accumulation as function of retinol density and diseases state (fibrotic versus healthy livers); healthy controls received intra-peritoneal injections of olive oil. Both healthy and fibrotic mice received a total dose of 0.8 mg NPs. (i) results expressed as mean ± SD NP concentration in the liver (ii) fold change in hepatic NP accumulation as function of fibrosis. ***extremely significant, **very significant, *significant, ns: not significant.

Once in the space of Disse, the NPs should gain preferential access into the HSCs. Several studies have confirmed the receptor-mediated uptake of Rt by HSCs [51,52]. In line with these previous reports, chitosan NP surface was covalently modified with Rt. We have previously demonstrated that the effectiveness of active targeting is highly dependent on targeting ligand density, where a higher ligand density does not always result in enhanced NP uptake by the target cell or organelle [26,53,54]. In general, very little work has been conducted to determine whether an optimal ligand density for cell surface targeting is required [49,55–61]. Interestingly, other studies looking into this aspect have in agreement with our findings, reported that a higher targeting density is not always favorable [49,55–60]. For such reason, we wanted to determine whether an optimal Rt density existed for NP targeting to HSCs. To do so, Rt was initially activated by CDI (Rt-CDI), to enable Rt binding to chitosan NP amine groups. Increasing concentrations of Rt-CDI were then added to the NPs, while monitoring the corresponding amount of Rt tagged. At 100% saturation; when any further increase in the concentration of Rt-CDI added failed to give an increase in amount tagged, NPs were assumed to have a high density of Rt; HRt-NPs having ≈ 0.86 molecules per nm^2. A low density of Rt was accordingly selected where LRt-NPs had ≈ 0.59 Rt molecules per nm^2. Interestingly, when added to freshly isolated primary HSCs, LRt-NPs showed higher uptake in comparison to unmodified NPs and to HRt-NPs. HSC transdifferentiate *in vitro* when cultured on plastic substrate in the presence of serum. This *in vitro* model is an acceptable tool to investigate the activation process [6,8,62]. When NPs were added to HSC that had been cultured on plastic for 4 days, Rt modified NPs (both LRt and HRt) failed to show any preferential uptake in comparison to unmodified NPs. The latter is in-line with the notion that unlike their activated form, quiescent HSCs express a high-affinity membrane receptor for RBP–retinol complex [51] and confirms that the higher uptake in quiescent HSCs was a function of Rt modification. The latter is also underpinned by the results obtained in HEK293 cells; while at the higher NP concentration (67 μg/ml) there was no significant difference between uptake of unmodified, LRt and HRt NPs, at the lower concentration, LRt-NPs showed lowest uptake whereas unmodified and HRt-NPs showed relatively higher uptake.

Sato et al. also developed vitamin A coupled liposomes for the delivery of siRNA against the rat homolog of human heat shock protein to HSCs [49]. The authors modified their liposomes with varying densities of vitamin A, i.e. 1:0.5, 1:1, 1:2, 1:4, 1:8, and 1:16 mol vitamin A: cationic lipid. Akin to the results reported herein, Sato et al. reported best results with the 1:2 ratio [49]. The reason as to why a lower Rt density provided better uptake than a higher one is not clear, however it is quite possible that the higher Rt densities results in tighter packing of Rt units on the surface of the NP causing steric interference, where the molecules existing in such close vicinity acquire a nonoptimal orientation for binding [56]. The latter is emphasized in the case of Rt, since HSCs uptake is mostly mediated via an intermediate complex in which the Rt binds to RBP [51]. The RBP is a small protein (21 kDa) for which the core is beta-barrel cavity used for Rt binding. For Rt binding, the apolar portion of Rt is buried with in such cavity and the Rt hydroxyl allocates to the protein surface [63]. These hydroxyls were used to link Rt to chitosan NP surface. This means that the space between the apolar parts of Rt molecules should be large enough to allow sufficient space for RBP binding.

In addition to the work reported by Sato et al., Pan and colleagues [50] also used Rt as a HSC targeting ligand. The authors developed Rt-lipid NPs for the delivery of silibinin to HSCs. However, in this case Rt was incorporated inside the NP matrix since it was added to the lipid phase during lipid NP preparation. This makes Rt unavailable at the NP surface or in a best-case scenario, randomly available at the surface. It is therefore no surprise that the authors reported no added benefit in terms of NP uptake or therapeutic effect when Rt-lipid NPs were incubated with HSCs [50]. Additionally, these particles were hydrophobic in nature and over 200 nm in size [50], and hence their liver accumulation might be attributed to Kupffer cell uptake. More importantly, even if Rt did make it to the surface, given the hydrophobic nature of the NPs developed, the apolar section of the Rt molecule (the one required for RBP binding) would be buried within the NP matrix and the Rt hydroxyls would be facing the outer aqueous phase also making the required link with RBP not possible. However, it is worth to note here that Sato et al. also modified their liposomes with Rt in a similar manner; by sonication of Rt with pre-formed liposomes, and hence the hydrophobic portion of Rt should theoretically have been buried with-in the liposomal bi-layer. In a similar approach to the work conducted herein, Zhang et al., tagged Rt using its hydroxyl groups [38]. In addition to the success of their formulation in treatment of fibrosis, the authors proved that NP uptake was in-fact facilitated via RBP [38].

The influence of Rt density on HSCs targeting was also obvious *in vivo*. When unmodified NPs, LRt-NPs and HRt-NPs were injected intravenously *via* the tail vein, LRt-NPs preferentially accumulated in fibrotic livers. Of more interest in this case, is the higher liver accumulation of LRt-NPs in fibrotic livers relative to healthy ones. Such increased uptake could not be simply attributed to the increased HSCs uptake by receptor mediated endocytosis on its own. This is mainly due to the fact that in fibrosis HSCs become activated downregulating the Rt receptor [6,8]. The latter was clearly demonstrated herein, when LRt-NPs were incubated with HSCs that have been cultured on plastic for 4 days. Instead, this preferential accumulation could be attributed to a cocktail of factors all working in favor of LRt-NPs. One significant player in such case, might be the change in serum protein make-up in liver disease. The serum protein profile has on numerous occasions been believed to change as a function of disease state [64,65]. The latter is also true for fibrosis, cirrhosis and hepatocellular carcinoma [64,66,67]. This in turn would result in a different composition of serum proteins constituting the protein corona forming around the NPs, which as detailed earlier is a major player in the NP bio-distribution. Since the types and quantities of the proteins involved in the protein corona formed is a function of the NP surface properties [19], the corona formed around unmodified NPs, LRt-NPs and HRt-NPs should theoretical be different. Additionally, it should be noted that RBP expression also changes in liver diseases. RBP expression has been reported to be significantly decreased with increasing nonalcoholic fatty liver diseases (NAFLD) severity for instance [68]. At the same time, other studies have shown an increase in serum RBP levels in patients with liver disease [69,70]. Interestingly, Zhang et al. demonstrated that Rt modified nanoparticles were selectively able to recruit RBP in their corona components and direct the NPs to HSCs [38]. The latter might be a possible mechanism explaining the accumulation LRt-NPs in fibrotic livers, where again the low Rt density offered maximum RBP recruiting ability. Once more, the latter is also underpinned by the *in vivo* NP accumulation trend observed in healthy livers, where LRt-NPs showed very low liver accumulation in comparison to unmodified and HRt-NPs. This again highlights the importance of targeting ligand density in NP targeting and stresses on the need for further studies to elucidate the implication of RBP expression levels on the preferential accumulation of LRt-NPs in fibrotic livers in comparison to healthy ones. More interestingly, the trend observed in NP uptake in HEK293 cells was also observed *in vivo*, where the liver accumulation of unmodified and HRt-NPs was not significantly different. Given the methodology used to study NP liver accumulation, NP sequestration in Kupffer cells could not be ruled out, since NP accumulation was studied by evaluating NP content in liver homogenates. However, Kupffer cell accumulation would not result in the trend observed in HEK293 cells *in vitro*.

With disregard to the mechanism involved, such preferential accumulation highlights the benefits of NP drug targeting and further minimizes off target effects, allowing the administration of drugs that would have otherwise been rendered un-administrable. One of these drugs is JQ1; thienotriazolodiazepine; a small molecule inhibitor of

BRD4 that has been reported to block HSC activation and significantly compromise their proliferative capacity [5]. In fact, Ding and colleagues have demonstrated the ability of JQ1 to reverse the fibrotic response in CCl_4-induced fibrosis in mouse models [5]. Similarly, we have demonstrated the ability of JQ1 loaded NPs to induce a reduction in α-SMA expression in a concertation dependent manner indicting a reduction in HSCs activation [29,71]. Cells were successfully treated with 1 and 10 μM of encapsulated JQ1. Treatment of cells with such concentrations in free unencapsulated from was not possible due to toxicity. Ding et al. reported a massive drop in viability (cell viability approaching 0%) when cells were treated with 2 μM JQ1 for 6 days and around 60% viability after 3 days only [5]. These results are very similar to what we observed with free JQ1 where at concentration of 1 and 10 μM, viable cells could not be harvested for the Western blot assay. However, when encapsulated in NPs, cells survived incubation with JQ1 for 7 days. In fact, the GAPDH band intensities obtained from wells that have been treated with JQ1 were quite similar to those obtained with unloaded NPs analyzed on the same gel (Fig. 5 B). It is noteworthy however that cell viability assays conducted using free JQ1 versus JQ1 NPs would provide deeper insights. The ability of the NPs to slowly release the loaded drug over time [54] is probably the main reason why such toxicity was not observed. On an *in vivo* level their ability to target the drug to HSCs as observed herein would also contribute to their improved safety profile. BET proteins control a plethora of transcriptional networks and are ubiquitously expressed across a variety of human cell types [17]. In fact, BRDs are key transcriptional regulators in inflammation, cancer, diabetes and cardiovascular diseases [72]. It is for such reason that care should be taken when these chromatin-dynamics modifying complexes are considered as therapeutic targets [73]. To complicate matters, given the structural similarity between different BRD proteins, most BET inhibitors lack specific actions. For instance, JQ1 was reported to exert an inhibitory effect on BRD2 and BRD3 as well [17,73,74]and hence is expected to exhibit a myriad of undesirable off target effects. Such lack of specificity might be the reason behind the drastic events reported in recent BET inhibitors cancer clinical trials [17,75]. Similar to JQ1, At loaded NPs have also successfully been able to reduce α-SMA expression in a concentration dependent manner, using drug concentrations (10 and 20 μM) that induced toxicity when used to treat cells in free from. Given their different modes of action, it is no surprise that co-treatment with JQ1 and At LRt-NPs showed a synergetic effect resulting in higher degree of α-SMA expression reduction.

Interestingly, given their Rt content, drugless unloaded Rt modified NPs also showed concentration dependent reduction in α-SMA expression when compared to unmodified NPs. It has been previously demonstrated that the *in vitro* treatment of HSCs with Rt could help maintain a quiescent phenotype and even induce reversion of phenotypic changes [76–78]. However, in such *in vitro* tests, given its hydrophobicity, Rt had to be administered as an ethanolic solution [76,77], complicating *in vivo* administration. When added to the NP surface, Rt-NPs are readily dispersible in aqueous media facilitating their *in vivo* intra-venous administration. The latter is complemented by results showing the hemocompatibility of our prepared NPs, where up to high concentrations (400 μg/mL) the NP did not induce any significant hemolysis or agglutination. In comparison to drugless unmodified NPs it is worth note that the effect of Rt modified unloaded NPs was most obvious with HRt-NPs (Fig. 5A). However, when compared to untreated cells, drugless LRt-NPs seem to reduce α-SMA expression as well (Fig. 5B). The observed effects in such cases could not be solely attributed to Rt content since chitosan itself may have a possible biological effect. Unfortunately, given the semi-quantitative nature of the assay used herein to quantify α-SMA expression, it could not be concluded whether the minute reduction in expression observed with unloaded, unmodified NPs (Supplementary Fig. S5) relative to untreated cells is in fact significant. Several reports have however described the inflammatory activity of chitosan [79,80]. At the same time other reports have described anti-inflammatory effect for chitosan [81,82]. It is quite possible at this point that the effect of chitosan is dependent on cell type and dose among other factors. In fact, it has been reported that chitosan shows an anti-inflammatory effect on M2 macrophages and a pro-inflammatory effect on M1 macrophages [83]. More interestingly, chitosan shows a dose-dependent effect in partially primed macrophages; anti-inflammatory at a low dose and pro-inflammatory at a high dose [83]. In the case of liver disease in particular, several studies have demonstrated the ant-inflammatory effects of chitosan [84–86]. In fact, very recently, it was demonstrated that chitosan exerts an anti-fibrotic effect in the a CCl_4 liver fibrosis animal model [87,88]. In particular, intravenous administration of chitosan resulted in a decrease in α-SMA expression [87]. However, in such cases, chitosan was administered as a polymeric solution and at much higher concentration than that used herein [87]. Further experiments investigating possible anti-fibrotic effects of unloaded, unmodified NPs and LRt-NPs *in vivo* would be insightful.

5. Conclusions

We have demonstrated that chitosan nanoparticles modified with a low density of Rt as a targeting ligand was able to show increased uptake in primary HSCs *in vitro* and increased accumulation in fibrotic liver *in vivo*, making them interesting vehicles for targeted drug delivery in liver fibrosis therapy. In fact, LRt-NPs have been successfully loaded with JQ1 and Atorvastatin and enabled HSC treatment with drug concentrations that were not suitable with free drug and hence resulting in a significant decrease in α-SMA expression; a marker for HSCs activation. While the *in vitro* results reported herein demonstrate the synergistic effect of At and JQ1 in delaying HSCs activation, an *in vivo* study conducted with a larger number of animals investigating the ability of JQ1 and At LRt-NPs in reversing fibrosis would be more insightful. The latter would be evaluated by histopathological evaluation of liver sections using by hematoxylin and eosin in addition to Sirius Red staining. On a more general note, this work in line our previous work [26,53,89], demonstrates the grave importance of targeting ligand density, where the mere inclusion of targeting ligand without careful optimization of targeting ligand density and orientation on the NP surface will not result in successful in active targeting. In fact, might increase drug concentration in an undesirable areas [89] aggravating the dilemma of off target effects.

Appendix A. Supplementary material

Supplementary data to this article can be found online at https://doi.org/10.1016/j.ejpb.2018.11.018.

References

[1] H.L. Reeves, S.L. Friedman, Activation of hepatic stellate cells—a key issue in liver fibrosis, Front Biosci. 7 (2002) 808–826.
[2] D. Schuppan, N.H. Afdhal, Liver cirrhosis, Lancet 371 (2008) 838–851.
[3] L. Wu, Q. Zhang, W. Mo, J. Feng, S. Li, J. Li, T. Liu, S. Xu, W. Wang, X. Lu, Q. Yu, K. Chen, Y. Xia, J. Lu, L. Xu, Y. Zhou, X. Fan, C. Guo, Quercetin prevents hepatic fibrosis by inhibiting hepatic stellate cell activation and reducing autophagy via the TGF-β1/Smads and PI3K/Akt pathways, Sci. Rep. 7 (2017) 9289.
[4] C.L. Wilson, J. Mann, M. Walsh, M.J. Perrugoria, F. Oakley, M.C. Wright, C. Brignole, D. Di Paolo, P. Perri, M. Ponzoni, Quiescent hepatic stellate cells functionally contribute to the hepatic innate immune response via TLR3, PLoS ONE 9 (2014) e83391.
[5] N. Ding, N. Hah, T.Y. Ruth, M.H. Sherman, C. Benner, M. Leblanc, M. He, C. Liddle, M. Downes, R.M. Evans, BRD4 is a novel therapeutic target for liver fibrosis, Proc. Natl. Acad. Sci. 112 (2015) 15713–15718.
[6] F. Tacke, R. Weiskirchen, Update on hepatic stellate cells: pathogenic role in liver fibrosis and novel isolation techniques, Expert Rev. Gastroenterol. Hepatol. 6 (2012) 67–80.
[7] K. Yu, N. Li, Q. Cheng, J. Zheng, M. Zhu, S. Bao, M. Chen, G. Shi, miR-96-5p prevents hepatic stellate cell activation by inhibiting autophagy via ATG7, J. Mol. Med. 96 (2018) 65–74.
[8] K. Rombouts, E. Kisanga, K. Hellemans, A. Wielant, D. Schuppan, A. Geerts, Effect of HMG-CoA reductase inhibitors on proliferation and protein synthesis by rat

hepatic stellate cells, J. Hepatol. 38 (2003) 564–572.
[9] J. Trebicka, M. Hennenberg, M. Odenthal, K. Shir, S. Klein, M. Granzow, A. Vogt, H.-P. Dienes, F. Lammert, J. Reichen, J. Heller, T. Sauerbruch, Atorvastatin attenuates hepatic fibrosis in rats after bile duct ligation via decreased turnover of hepatic stellate cells, J. Hepatol. 53 (2000) 702–712.
[10] T.G. Simon, L.Y. King, H. Zheng, R.T. Chung, Statin use is associated with a reduced risk of fibrosis progression in chronic hepatitis C, J. Hepatol. 62 (2015) 18–23.
[11] J.G. Abraldes, A. Albillos, R. Bañares, J. Turnes, R. González, J.C. García-Pagán, J. Bosch, Simvastatin lowers portal pressure in patients with cirrhosis and portal hypertension: a randomized controlled trial, Gastroenterology 136 (2009) 1651–1658.
[12] J. Meloche, F. Potus, M. Vaillancourt, A. Bourgeois, I. Johnson, L. Deschamps, S. Chabot, G. Ruffenach, S. Henry, S. Breuils-Bonnet, Bromodomain-containing protein 4 novelty and significance: the epigenetic origin of pulmonary arterial hypertension, Circul. Res. 117 (2015) 525–535.
[13] J.J. Barrow, E. Balsa, F. Verdeguer, C.D. Tavares, M.S. Soustek, L.R. Hollingsworth IV, M. Jedrychowski, R. Vogel, J.A. Paulo, J. Smeitink, Bromodomain inhibitors correct bioenergetic deficiency caused by mitochondrial disease complex I mutations, Mol. Cell 64 (2016) 163–175.
[14] S.R. Floyd, M.E. Pacold, Q. Huang, S.M. Clarke, F.C. Lam, I.G. Cannell, B.D. Bryson, J. Rameseder, M.J. Lee, E.J. Blake, The bromodomain protein Brd4 insulates chromatin from DNA damage signalling, Nature 498 (2013) 246.
[15] E. Korb, M. Herre, I. Zucker-Scharff, R.B. Darnell, C.D. Allis, BET protein Brd4 activates transcription in neurons and BET inhibitor Jq1 blocks memory in mice, Nat. Neurosci. 18 (2015) 1464.
[16] S. Jostes, D. Nettersheim, M. Fellermeyer, S. Schneider, F. Hafezi, F. Honecker, V. Schumacher, M. Geyer, G. Kristiansen, H. Schorle, The bromodomain inhibitor JQ1 triggers growth arrest and apoptosis in testicular germ cell tumours in vitro and in vivo, J. Cell Mol. Med. 21 (2017) 1300–1314.
[17] G. Andrieu, A.C. Belkina, G.V. Denis, Clinical trials for BET inhibitors run ahead of the science, Drug Discov. Today: Technol. 19 (2016) 45–50.
[18] S. Alghamdi, I. Khan, N. Beeravolu, C. McKee, B. Thibodeau, G. Wilson, G.R. Chaudhry, BET protein inhibitor JQ1 inhibits growth and modulates WNT signaling in mesenchymal stem cells, Stem Cell Res. Ther. 7 (2016) 22.
[19] S.N. Tammam, H.M. Azzazy, A. Lamprecht, Biodegradable particulate carrier formulation and tuning for targeted drug delivery, J. Biomed. Nanotechnol. 11 (2015) 555–577.
[20] H.-T. Schon, M. Bartneck, E. Borkham-Kamphorst, J. Nattermann, T. Lammers, F. Tacke, R. Weiskirchen, Pharmacological intervention in hepatic stellate cell activation and hepatic fibrosis, Front. Pharmacol. 7 (2016).
[21] F. Braet, E. Wisse, Structural and functional aspects of liver sinusoidal endothelial cell fenestrae: a review, Comp. Hepatol. 1 (2002) 1.
[22] V.C. Cogger, J.N. O'Reilly, A. Warren, Le Couteur DG. A standardized method for the analysis of liver sinusoidal endothelial cells and their fenestrations by scanning electron microscopy, J. Visual. Exp.: JoVE. (2015).
[23] Y. Iwakiri, V. Shah, D.C. Rockey, Vascular pathobiology in chronic liver disease and cirrhosis–current status and future directions, J. Hepatol. 61 (2014) 912–924.
[24] L.D. DeLeve, Liver sinusoidal endothelial cells in hepatic fibrosis, Hepatology (Baltimore, MD) 61 (2015) 1740–1746.
[25] T. Mori, T. Okanoue, Y. Sawa, N. Hori, M. Ohta, K. Kagawa, Defenestration of the sinusoidal endothelial cell in a rat model of cirrhosis, Hepatology 17 (1993) 891–897.
[26] S.N. Tammam, H.M.E. Azzazy, H.G. Breitinger, A. Lamprecht, Chitosan nanoparticles for nuclear targeting: the effect of nanoparticle size and nuclear localization sequence density, Mol. Pharm. 12 (2015) 4277–4289.
[27] Y. Zhou, J. Li, F. Lu, J. Deng, J. Zhang, P. Fang, X. Peng, S.-F. Zhou, A study on the hemocompatibility of dendronized chitosan derivatives in red blood cells, Drug Design, Develop. Therapy 9 (2015) 2635–2645.
[28] R.B. Ford, E.M. Mazzaferro, Section 5 – Laboratory Diagnosis and Test Protocols. Kirk & Bistner's Handbook of Veterinary Procedures and Emergency Treatment, Ninth Edition, W.B. Saunders, Saint Louis, 2012, pp. 551–634.
[29] S. Weiskirchen, C.G. Tag, S. Sauer-Lehnen, F. Tacke, R. Weiskirchen, Isolation and Culture of Primary Murine Hepatic Stellate Cells. Fibrosis, Springer, 2017, pp. 165–191.
[30] S.N. Tammam, H.M. Azzazy, A. Lamprecht, A high throughput method for quantification of cell surface bound and internalized chitosan nanoparticles, Int. J. Biol. Macromol. 81 (2015) 858–866.
[31] F.L. Graham, J. Smiley, W. Russell, R. Nairn, Characteristics of a human cell line transformed by DNA from human adenovirus type 5, J. Gen. Virol. 36 (1977) 59–72.
[32] S. Klein, J. Klösel, R. Schierwagen, C. Körner, M. Granzow, S. Huss, I.G.R. Mazar, S. Weber, P.F. Van Den Ven, U. Pieper-Fürst, Atorvastatin inhibits proliferation and apoptosis, but induces senescence in hepatic myofibroblasts and thereby attenuates hepatic fibrosis in rats, Lab. Invest. 92 (2012) 1440.
[33] E. Borkham-Kamphorst, B.T. Steffen, E. Van de Leur, L. Tihaa, U. Haas, M.M. Woitok, S.K. Meurer, R. Weiskirchen, Adenoviral CCN gene transfers induce in vitro and in vivo endoplasmic reticulum stress and unfolded protein response, Biochimica et Biophysica Acta (BBA)-Mol. Cell Res. 1863 (2016) 2604–2612.
[34] S.C. Yanguas, B. Cogliati, J. Willebrords, M. Maes, I. Colle, B. van den Bossche, C.P.M.S. de Oliveira, W. Andraus, V.A.F. Alves, I. Leclercq, M. Vinken, Experimental models of liver fibrosis, Arch. Toxicol. 90 (2016) 1025–1048.
[35] J.E. Adrian, J.A. Kamps, G.L. Scherphof, D.K. Meijer, Reker-Smit C, Terpstra P, Poelstra K. A novel lipid-based drug carrier targeted to the non-parenchymal cells, including hepatic stellate cells, in the fibrotic livers of bile duct ligated rats, Biochimica et Biophysica Acta (BBA)-Biomembranes 1768 (2007) 1430–1439.
[36] L. Giannitrapani, M. Soresi, M.L. Bondì, G. Montalto, M. Cervello, Nanotechnology applications for the therapy of liver fibrosis, World J. Gastroenterol.: WJG 20 (2014) 7242.
[37] S. Tenzer, D. Docter, J. Kuharev, A. Musyanovych, V. Fetz, R. Hecht, F. Schlenk, D. Fischer, K. Kiouptsi, C. Reinhardt, K. Landfester, H. Schild, M. Maskos, S.K. Knauer, R.H. Stauber, Rapid formation of plasma protein corona critically affects nanoparticle pathophysiology, Nat. Nanotechnol. 8 (2013) 772.
[38] Z. Zhang, C. Wang, Y. Zha, W. Hu, Z. Gao, Y. Zang, J. Chen, J. Zhang, L. Dong, Corona-directed nucleic acid delivery into hepatic stellate cells for liver fibrosis therapy, ACS Nano 9 (2015) 2405–2419.
[39] S. Tammam, S. Mathur, N. Afifi, Preparation and biopharmaceutical evaluation of tacrolimus loaded biodegradable nanoparticles for liver targeting, J. Biomed. Nanotechnol. 8 (2012) 439–449.
[40] Z. Amoozgar, J. Park, Q. Lin, Y. Yeo, Low molecular-weight chitosan as a pH-sensitive stealth coating for tumor-specific drug delivery, Mol. Pharm. 9 (2012) 1262–1270.
[41] J.E. Adrian, K. Poelstra, G.L. Scherphof, G. Molema, D.K. Meijer, C. Reker-Smit, H.W. Morselt, J.A. Kamps, Interaction of targeted liposomes with primary cultured hepatic stellate cells: Involvement of multiple receptor systems, J. Hepatol. 44 (2006) 560–567.
[42] S.-L. Du, H. Pan, W.-Y. Lu, J. Wang, J. Wu, J.-Y. Wang, Cyclic Arg-Gly-Asp peptide-labeled liposomes for targeting drug therapy of hepatic fibrosis in rats, J. Pharmacol. Exp. Ther. 322 (2007) 560–568.
[43] F. Li, Li Q-h, Wang J-y, Zhan C-y, C. Xie, Lu W-y. Effects of interferon-gamma liposomes targeted to platelet-derived growth factor receptor–beta on hepatic fibrosis in rats, J. Control. Release 159 (2012) 261–270.
[44] J. Yang, Y. Hou, G. Ji, Z. Song, Y. Liu, G. Dai, Y. Zhang, J. Chen, Targeted delivery of the RGD-labeled biodegradable polymersomes loaded with the hydrophilic drug oxymatrine on cultured hepatic stellate cells and liver fibrosis in rats, Eur. J. Pharm. Sci. 52 (2014) 180–190.
[45] J.S. Smith, J. Tian, J.N. Lozier, A.P. Byrnes, Severe pulmonary pathology after intravenous administration of vectors in cirrhotic rats, Mol. Ther. 9 (2004) 932–941.
[46] B. Pelaz, P. del Pino, P. Maffre, R. Hartmann, M. Gallego, S. Rivera-Fernandez, J.M. de la Fuente, G.U. Nienhaus, W.J. Parak, Surface functionalization of nanoparticles with polyethylene glycol: effects on protein adsorption and cellular uptake, ACS Nano 9 (2015) 6996–7008.
[47] R. Rattan, S. Bhattacharjee, H. Zong, C. Swain, M.A. Siddiqui, S.H. Visovatti, Y. Kanthi, S. Desai, D.J. Pinsky, S.N. Goonewardena, Nanoparticle-macrophage interactions: a balance between clearance and cell-specific targeting, Bioorg. Med. Chem. 25 (2017) 4487–4496.
[48] S.J. Soenen, B.B. Manshian, A.M. Abdelmonem, J.M. Montenegro, S. Tan, L. Balcaen, F. Vanhaecke, A.R. Brisson, W.J. Parak, S.C. De Smedt, The cellular interactions of PEGylated gold nanoparticles: effect of PEGylation on cellular uptake and cytotoxicity, Part. Part. Syst. Char. 31 (2014) 794–800.
[49] Y. Sato, K. Murase, J. Kato, M. Kobune, T. Sato, Y. Kawano, R. Takimoto, K. Takada, K. Miyanishi, T. Matsunaga, Resolution of liver cirrhosis using vitamin A–coupled liposomes to deliver siRNA against a collagen-specific chaperone, Nat. Biotechnol. 26 (2008) 431.
[50] T.-L. Pan, P.-W. Wang, C.-F. Hung, I.A. Aljuffali, Y.-S. Dai, J.-Y. Fang, The impact of retinol loading and surface charge on the hepatic delivery of lipid nanoparticles, Colloids Surf., B 141 (2016) 584–594.
[51] V.A. Fortuna, R.B. Martucci, L.C. Trugo, R. Borojevic, Hepatic stellate cells uptake of retinol associated with retinol-binding protein or with bovine serum albumin, J. Cell. Biochem. 90 (2003) 792–805.
[52] H. Senoo, S.R. Smeland, L. Malaba, T. Bjerknes, E. Stang, N. Roos, T. Berg, K.R. Norum, R. Blomhoff, Transfer of retinol-binding protein from HepG2 human hepatoma cells to cocultured rat stellate cells, Proc. Natl. Acad. Sci. 90 (1993) 3616–3620.
[53] S.N. Tammam, H.M. Azzazy, A. Lamprecht, The effect of nanoparticle size and NLS density on nuclear targeting in cancer and normal cells; impaired nuclear import and aberrant nanoparticle intracellular trafficking in glioma, J. Control. Release 253 (2017) 30–36.
[54] Y. Abbas, H.M.E. Azzazy, S. Tammam, A. Lamprecht, M.E. Ali, A. Schmidt, S. Sollazzo, S. Mathur, Development of an inhalable, stimuli-responsive particulate system for delivery to deep lung tissue, Colloids Surf., B 146 (2016) 19–30.
[55] Z. Poon, S. Chen, A.C. Engler, Lee Hi, E. Atas, G. von Maltzahn, S.N. Bhatia, P.T. Hammond, Ligand-clustered "Patchy" nanoparticles for modulated cellular uptake and in vivo tumor targeting, Angew. Chem. Int. Ed. 49 (2010) 7266–7270.
[56] D.R. Elias, A. Poloukhtine, V. Popik, A. Tsourkas, Effect of ligand density, receptor density, and nanoparticle size on cell targeting, Nanomed. Nanotechnol. Biol. Med. 9 (2013) 194–201.
[57] K. Kawano, Y. Maitani, Effects of polyethylene glycol spacer length and ligand density on folate receptor targeting of liposomal Doxorubicin in vitro, J. Drug Deliv. (2011;2011.).
[58] J.M. Saul, A. Annapragada, J.V. Natarajan, R.V. Bellamkonda, Controlled targeting of liposomal doxorubicin via the folate receptor in vitro, J. Control. Release 92 (2003) 49–67.
[59] K.B. Ghaghada, J. Saul, J.V. Natarajan, R.V. Bellamkonda, A.V. Annapragada, Folate targeting of drug carriers: a mathematical model, J. Control. Release 104 (2005) 113–128.
[60] J. Wang, S. Tian, R.A. Petros, M.E. Napier, J.M. DeSimone, The complex role of multivalency in nanoparticles targeting the transferrin receptor for cancer therapies, J. Am. Chem. Soc. 132 (2010) 11306–11313.
[61] C. Dalal, A. Saha, N.R. Jana, Nanoparticle multivalency directed shifting of cellular uptake mechanism, J. Phys. Chem. C 120 (2016) 6778–6786.
[62] A.L. Olsen, S.A. Bloomer, E.P. Chan, M.D. Gaça, P.C. Georges, B. Sackey, M. Uemura, P.A. Janmey, R.G. Wells, Hepatic stellate cells require a stiff

environment for myofibroblastic differentiation, Am. J. Physiol-Gastrointestinal Liver Physiol. 301 (2011) G110–G118.
[63] G. Zanotti, R. Berni, Plasma Retinol-Binding Protein: Structure and Interactions with Retinol, Retinoids, and Transthyretin. Vitamins & Hormones, Academic Press, 2004, pp. 271–295.
[64] L.N. Bell, J.L. Theodorakis, R. Vuppalanchi, R. Saxena, K.G. Bemis, M. Wang, N. Chalasani, Serum proteomics and biomarker discovery across the spectrum of nonalcoholic fatty liver disease, Hepatology (Baltimore, MD) 51 (2010) 111–120.
[65] E.F. Petricoin III, A.M. Ardekani, B.A. Hitt, P.J. Levine, V.A. Fusaro, S.M. Steinberg, G.B. Mills, C. Simone, D.A. Fishman, E.C. Kohn, Use of proteomic patterns in serum to identify ovarian cancer, Lancet 359 (2002) 572–577.
[66] V.R. Mas, D.G. Maluf, K.J. Archer, K. Yanek, K. Bornstein, R.A. Fisher, Proteomic analysis of HCV cirrhosis and HCV-induced HCC: Identifying biomarkers for monitoring HCV-cirrhotic patients awaiting liver transplantation, Transplantation 87 (2009) 143–152.
[67] R. Chaerkady, H.C. Harsha, A. Nalli, M. Gucek, P. Vivekanandan, J. Akhtar, R.N. Cole, J. Simmers, R.D. Schulick, S. Singh, M. Torbenson, A. Pandey, P.J. Thuluvath, A quantitative proteomic approach for identification of potential biomarkers in hepatocellular carcinoma, J. Proteome Res. 7 (2008) 4289–4298.
[68] V. Nobili, N. Alkhouri, A. Alisi, S. Ottino, R. Lopez, M. Manco, A.E. Feldstein, Retinol-binding protein 4: a promising circulating marker of liver damage in pediatric nonalcoholic fatty liver disease, Clin. Gastroenterol. Hepatol. 7 (2009) 575–579.
[69] J.A. Seo, N.H. Kim, S.Y. Park, H.Y. Kim, O.H. Ryu, K.W. Lee, J. Lee, D.L. Kim, K.M. Choi, S.H. Baik, D.S. Choi, S.G. Kim, Serum retinol-binding protein 4 levels are elevated in non-alcoholic fatty liver disease, Clin. Endocrinol. 68 (2008) 555–560.
[70] W.-T. Chen, M.-S. Lee, C.-L. Chang, C.-T. Chiu, M.-L. Chang, Retinol-binding protein-4 expression marks the short-term mortality of critically ill patients with underlying liver disease: Lipid, but not glucose, matters, Sci. Rep. 7 (2017) 2881.
[71] C.-M. Chu, W.-C. Shyu, Y.-F. Liaw, Comparative studies on expression of α-smooth muscle actin in hepatic stellate cells in chronic hepatitis B and C, Dig. Dis. Sci. 53 (2008) 1364–1369.
[72] M. Pérez-Salvia, M. Esteller, Bromodomain inhibitors and cancer therapy: from structures to applications, Epigenetics 12 (2017) 323–339.
[73] A.C. Belkina, G.V. Denis, BET domain co-regulators in obesity, inflammation and cancer, Nat. Rev. Cancer 12 (2012) 465–477.
[74] P. Filippakopoulos, J. Qi, S. Picaud, Y. Shen, W.B. Smith, O. Fedorov, E.M. Morse, T. Keates, T.T. Hickman, I. Felletar, M. Philpott, S. Munro, M.R. McKeown, Y. Wang, A.L. Christie, N. West, M.J. Cameron, B. Schwartz, T.D. Heightman, N. La Thangue, C.A. French, O. Wiest, A.L. Kung, S. Knapp, J.E. Bradner, Selective inhibition of BET bromodomains, Nature 468 (2010) 1067–1073.
[75] D. Butler, E. Callaway, Scientists in the dark after fatal French clinical trial: knowledge about the drug's structure would help researchers understand what happened, Nature 529 (2016) 263–265.
[76] B. Davis, R. Kramer, N. Davidson, Retinoic acid modulates rat Ito cell proliferation, collagen, and transforming growth factor beta production, J. Clin. Investig. 86 (1990) 2062–2070.
[77] B. Davis, U.R. Rapp, N. Davidson, Retinoic acid and transforming growth factor beta differentially inhibit platelet-derived-growth-factor-induced Ito-cell activation, Biochem. J 278 (1991) 43.
[78] T.F. Lee, K.M. Mak, O.R.I. Rackovsky, Y.-L. Lin, A.J. Kwong, J.C. Loke, S.L. Friedman, Downregulation of hepatic stellate cell activation by retinol and palmitate mediated by adipose differentiation-related protein (ADRP), J. Cell. Physiol. 223 (2010) 648–657.
[79] P. Zhang, W. Liu, Y. Peng, B. Han, Y. Yang, Toll like receptor 4 (TLR4) mediates the stimulating activities of chitosan oligosaccharide on macrophages, Int. Immunopharmacol. 23 (2014) 254–261.
[80] Y. Dang, S. Li, W. Wang, S. Wang, M. Zou, Y. Guo, J. Fan, Y. Du, J. Zhang, The effects of chitosan oligosaccharide on the activation of murine spleen CD11c+ dendritic cells via Toll-like receptor 4, Carbohydr. Polym. 83 (2011) 1075–1081.
[81] J. Tu, Y. Xu, J. Xu, Y. Ling, Y. Cai, Chitosan nanoparticles reduce LPS-induced inflammatory reaction via inhibition of NF-κB pathway in Caco-2 cells, Int. J. Biol. Macromol. 86 (2016) 848–856.
[82] G. Kerch, The potential of chitosan and its derivatives in prevention and treatment of age-related diseases, Mar Drugs 13 (2015) 2158–2182.
[83] D. Fong, C. Hoemann, Chitosan immunomodulatory properties: prespective on the impact of structural propertie and dosage, Future Sci. 4 (2017).
[84] O. AboZaid, O. AbdEl-Hamid, S. Atwa, Hypolipidemic and anti-inflammatory effect of chitosan in experimental induced non -alcoholic fatty liver disease in rats, Benha Veterinary Med. J. 28 (2015) 155–165.
[85] E. Ozcelik, S. Uslu, N. Erkasap, H. Karimi, Protective effect of chitosan treatment against acetaminophen induced hepatotoxcity, Kaohsiung J. Med. Sci. 30 (2014) 286–290.
[86] M. Yu, Y. Wang, T. Jiang, Z. Lv, Effects of sulfate chitosan derivatives on non-alcoholic fatty liver disease, J. Ocean Univ. China 13 (2014) 531–537.
[87] Z.-F. Wang, M.-Y. Wang, D.-H. Yu, Y. Zhao, H.-M. Xu, S. Zhong, W.-Y. Sun, Y.-F. He, J.-Q. Niu, P.-J. Gao, H.-J. Li, Therapeutic effect of chitosan on CCl(4)-induced hepatic fibrosis in rats, Mol. Med. Rep. 18 (2018) 3211–3218.
[88] E. Denshary, A. Aljawish, A. El-Nekeety, N. Hassan, R. Saleh, B. Rihn, M. Abdel-Wahhab, Possible synergistic effect and antioxidant properties of chitosan nanoparticles and quercetin against carbon tetrachloride induced hepatotoxcity in rats, Soft Nanosci. Lett. 5 (2) (2015), https://doi.org/10.4236/snl.2015.52005.
[89] S.N. Tammam, H.M.E. Azzazy, A. Lamprecht, Nuclear and cytoplasmic delivery of lactoferrin in glioma using chitosan nanoparticles: cellular location dependent-action of lactoferrin, Eur. J. Pharm. Biopharm. 129 (2018) 74–79.